On the overlap dynamics of multi-state neural networks with a finite number of patterns

1992 J. Phys. A: Math. Gen. 25 2859

(http://iopscience.iop.org/0305-4470/25/10/014)

J. Phys. A: Math. Gen. 25 (1992) 2859-2872. Printed in the UK

On the overlap dynamics of multi-state neural networks with a finite number of patterns

D Bollé†, P Dupont‡ and B Vinck

Instituut voor Theoretische Fysica, Katholieke Universiteit Leuven, B-3001 Leuven, Belgium

Received 9 December 1991

Abstract. Neural networks with multi-state neurons are studied in the case of low loading. For symmetric couplings satisfying a certain positivity condition, a Lyapunov function is shown to exist in the space of overlaps between the instantaneous microscopic state of the system and the learned patterns. Furthermore, an algorithm is derived for zero temperature to determine all the fixed points. As an illustration, the three-state model is worked out explicitly for Hebbian couplings. For finite temperature the time evolution of the overlap is studied for couplings which need not be symmetric. The stability properties are discussed in detail for the three-state model. For asymmetric couplings limit-cycle behaviour is shown to be possible.

1. Introduction

Neural networks with multi-state neurons have recently received a lot of attention [1-16]. Thereby the ability to store and retrieve so-called grey-toned patterns has been investigated. One of the models that has been discussed in [4-8, 11, 12] is based upon the Q-Ising spin glass. For this model, the capacity-temperature phase diagram has been determined using the pseudo-inverse rule [7]. Furthermore, an analysis of the space of couplings has led to the distribution of the local fields, the critical storage capacity and the minimal number of errors in the case of overloading [11, 12]. Finally, concerning the dynamics, for three-state $(-1, 0, 1)$ neurons a numerical analysis from the point of view of information processing has been given for the fully connected version at zero temperature [4] and analytic results have been presented for the non-symmetric highly dilute version of this model [5].

In this paper, we consider the fully connected Q-Ising spin glass neural network with self-coupling at zero and finite temperature, in the case of low loading (i.e. for a finite number of patterns). In particular, for symmetric couplings satisfying a certain positivity condition, a Lyapunov function is derived for the dynamics in the space of overlaps between the instantaneous microscopic state of the system and the learned patterns. At zero temperature this leads to an algorithm to determine all the fixed points. For finite temperature the dynamical evolution of the overlap is studied for couplings which need not be symmetric. Retrieval states, symmetric and asymmetric states and limit-cycle behaviour are discussed. The results are worked out explicitly

† e-mail: FGBDA18@BLEKUL11.BITNET.
‡ Present address: University Hospital Gasthuisberg, Department of Nuclear Medicine, B-3000 Leuven, Belgium.

0305-4470/92/102859+14$04.50

for the three-state model with a small number of patterns. They are compared with the findings of a similar analysis made for the Hopfield model [17-22] and for the Potts model [9, 20, 21].

The rest of the paper is organized as follows. In section 2 we describe the model and derive in mean field approximation the free energy and fixed-point equations for the overlap parameters. In section 3 we study the system at zero temperature for symmetric couplings satisfying a certain positivity condition. Here the approach of Procesi and Tirozzi [18] is generalized: we prove that the free energy is a Lyapunov function and formulate an algorithm to find all the fixed points of the dynamics. As an example, we discuss the $Q=3$ model with $p=2$ patterns for Hebbian couplings. Besides the retrieval states, the existence of symmetric and asymmetric states is studied as a function of b, an extra parameter introduced to control the relative importance of the neuron states which are low in absolute value. Section 4 deals with the system at arbitrary temperature for couplings which need not be symmetric. Although the neuron dynamics is now stochastic, the overlap dynamics is deterministic. This leads to the derivation of flow equations for the overlap. Again, the $Q=3$ model with $p=2$ patterns is studied in detail. Limit-cycle behaviour is shown to be possible for asymmetric couplings. Finally, in section 5 the conclusions are presented.

2. The model

Consider a fully connected network with N neurons which can take values in a set $\Sigma=\{-1=s_1<s_2<\ldots<s_{Q-1}<s_Q=+1\}$ where the elements have mean 0. A state of the system will be denoted by $\sigma=(\sigma(1),\ldots,\sigma(N))$. We want to store p patterns $\{\xi_i^\mu\}$, $i=1,\ldots,N$, $\mu=1,\ldots,p$, where ξ_i^μ are independent random variables with the same uniform distribution as the neurons. We study the following Hamiltonian:

$$H(b)=-\tfrac{1}{2}\sum_{i,j=1}^{N} J_{ij}\sigma(i)\sigma(j)+b\sum_{i=1}^{N}\sigma(i)^2. \tag{1}$$

The synaptic couplings J_{ij} are given by

$$J_{ij}=\frac{1}{NC}\sum_{\mu,\nu=1}^{p}\xi_i^\mu A_{\mu\nu}\xi_j^\nu \tag{2}$$

where A is an invertible symmetric $p\times p$ matrix and where $C=\langle\!\langle \xi^2\rangle\!\rangle$ with $\langle\!\langle\cdot\rangle\!\rangle$ denoting the average over the distribution of the patterns. For $A=1$, equation (2) reduces to the Hebb rule. Note that we do allow self-coupling. The parameter $b>0$ is introduced as an additional degree of freedom in order to control the relative importance of states which are low in absolute value. The local field h_i in neuron i is defined as

$$h_i(\sigma)=\sum_{j=1}^{N} J_{ij}\sigma(j). \tag{3}$$

Using standard techniques [17] the free energy at temperature T is calculated in the limit $N\to\infty$ as

$$F(T,m)=\frac{C}{2}m\cdot Am-T\left\langle\!\!\left\langle \ln\sum_{k=1}^{Q}\exp\left[\frac{1}{T}(\xi\cdot Ams_k-bs_k^2)\right]\right\rangle\!\!\right\rangle \tag{4}$$

with $\boldsymbol{\xi}=(\xi^1,\ldots,\xi^p)$. The variables $\boldsymbol{m}=(m^1,\ldots,m^p)$ are introduced through the saddle-point method. They satisfy the following fixed-point equation:

$$\boldsymbol{m}=\frac{1}{C}\left\langle\!\!\left\langle \boldsymbol{\xi}\frac{\sum_{k=1}^{Q} s_k \exp[(1/T)(\boldsymbol{\xi}\cdot A\boldsymbol{m}s_k - bs_k^2)]}{\sum_{k=1}^{Q}\exp[(1/T)(\boldsymbol{\xi}\cdot A\boldsymbol{m}s_k - bs_k^2)]}\right\rangle\!\!\right\rangle. \tag{5}$$

3. Zero temperature dynamics

In this section the results of [18] are generalized to the multi-state model discussed in section 2 with A strictly positive.

Suppose the state of the network at time t is $\boldsymbol{\sigma}$. The state of neuron i after the next time step, i.e. at $t+\Delta t$, is

$$U\boldsymbol{\sigma}(i)=g(h_i(\boldsymbol{\sigma})) \tag{6}$$

where g is the input-output function:

$$g(x)=\begin{cases} s_1=-1 & \text{if } x<b(s_1+s_2) \\ s_k & \text{if } b(s_{k-1}+s_k)\leqslant x<b(s_k+s_{k+1}) \qquad k=2,\ldots,Q-1 \\ s_Q=+1 & \text{if } b(s_{Q-1}+s_Q)\leqslant x. \end{cases} \tag{7}$$

We define the overlap between the instantaneous microscopic state of the system, $\boldsymbol{\sigma}$, and pattern $\{\xi_i^\mu\}$, $i=1,\ldots,N$, as

$$m^\mu=\frac{1}{NC}\sum_{i=1}^{N}\xi_i^\mu\sigma(i). \tag{8}$$

The neuron dynamics induces in a natural way a dynamics in the space of overlaps:

$$U\boldsymbol{m}=\frac{1}{NC}\sum_{i=1}^{N}\boldsymbol{\xi}_i(U\boldsymbol{\sigma})(i) \tag{9}$$

with $\boldsymbol{\xi}_i=(\xi_i^1,\ldots,\xi_i^p)$. Using the fact that $h_i(\boldsymbol{\sigma})=\boldsymbol{\xi}_i\cdot A\boldsymbol{m}$, we get by the law of large numbers

$$U\boldsymbol{m}=\frac{1}{C}\langle\!\langle \boldsymbol{\xi}\, g(\boldsymbol{\xi}\cdot A\boldsymbol{m})\rangle\!\rangle. \tag{10}$$

In addition, the limit $T\to 0$ of the fixed-point equation (5) reads

$$\boldsymbol{m}=\frac{1}{C}\langle\!\langle \boldsymbol{\xi}\, s_{\max}(\boldsymbol{\xi}\cdot A\boldsymbol{m})\rangle\!\rangle \tag{11}$$

where

$$s_{\max}(\boldsymbol{\xi}\cdot A\boldsymbol{m})=\max_{s\in\Sigma}(\boldsymbol{\xi}\cdot A\boldsymbol{m}s-bs^2). \tag{12}$$

It is easy to show that

$$s_{\max}(\boldsymbol{\xi}\cdot A\boldsymbol{m})=g(\boldsymbol{\xi}\cdot A\boldsymbol{m}). \tag{13}$$

Hence the variables $\boldsymbol{m}$, appearing in (4) and (5) can be interpreted as the overlap with the patterns. This means that the overlap (8) is the correct order parameter describing the correlations between the state of the system and the patterns. We must be aware

that (8) attains values up to $m_{\max} = \langle\langle |\xi| \rangle\rangle$, which exceeds one if $Q > 3$, and that it does not measure the quality of retrieval. A better quantity to measure the retrieval quality of a network is the Hamming distance between the instantaneous microscopic state and the patterns:

$$d^\mu = \frac{1}{4N} \sum_{i=1}^{N} (\sigma(i) - \xi_i^\mu)^2. \tag{14}$$

Here we observe that in a fixed point, where $\sigma(i) = g(\xi_i \cdot A\boldsymbol{m})$, we obtain

$$d^\mu = \tfrac{1}{4}\langle\langle (g(\xi \cdot A\boldsymbol{m}) - \xi^\mu)^2 \rangle\rangle. \tag{15}$$

So in the following we concentrate on the overlap $\boldsymbol{m}$.

Next we show that the zero temperature limit of the free energy (4) is a Lyapunov function for the overlap dynamics

$$E(\boldsymbol{m}) \equiv \lim_{T \to 0} F(T, \boldsymbol{m}) \tag{16}$$

$$= \frac{C}{2} \boldsymbol{m} \cdot A\boldsymbol{m} - \langle\langle \xi \cdot A\boldsymbol{m}\, g(\xi \cdot A\boldsymbol{m}) \rangle\rangle + b\langle\langle g^2(\xi \cdot A\boldsymbol{m}) \rangle\rangle. \tag{17}$$

Consider a vector $\zeta \in \Sigma^{Q^p}$. Because there are exactly Q^p vectors ξ we can label the components of ζ by the ξs. We then define

$$G_\zeta = \{\boldsymbol{m} \in \mathbb{R}^p \mid g(\xi \cdot A\boldsymbol{m}) = \zeta_\xi\}. \tag{18}$$

This gives a partition of the space of overlaps in disjoint convex regions.

If $\boldsymbol{m} \in G_\zeta$ and $\boldsymbol{m}' \in G_\zeta$ then $U\boldsymbol{m} = U\boldsymbol{m}'$. Furthermore, if $\boldsymbol{m} \in G_\zeta$ and $U\boldsymbol{m} \in G_\zeta$ then $U\boldsymbol{m}$ is a fixed point.

Define now for each ζ the following function on the space of overlaps:

$$Q_\zeta(\boldsymbol{v}) = \frac{C}{2} \boldsymbol{v} \cdot A\boldsymbol{v} - C\boldsymbol{v} \cdot A\boldsymbol{v}_\zeta + b\langle\langle \zeta_\xi^2 \rangle\rangle \tag{19}$$

with $\boldsymbol{v}_\zeta = U\boldsymbol{m}$ for an arbitrary $\boldsymbol{m} \in G_\zeta$. It is clear that on G_ζ, $Q_\zeta(\cdot)$ and $E(\cdot)$ agree. Moreover, $Q_\zeta(\cdot)$ has its absolute minimum in $\boldsymbol{v}_\zeta$ because $Q_\zeta(\boldsymbol{v}) - Q_\zeta(\boldsymbol{v}_\zeta) = (C/2)(\boldsymbol{v} - \boldsymbol{v}_\zeta) \cdot A(\boldsymbol{v} - \boldsymbol{v}_\zeta)$. Comparing $Q_\zeta(\boldsymbol{v}_\zeta)$ and $E(\boldsymbol{v}_\zeta)$ we get

$$Q_\zeta(\boldsymbol{v}_\zeta) - E(\boldsymbol{v}_\zeta) = \langle\langle (\zeta_\xi^+ - \zeta_\xi)(\xi \cdot A\boldsymbol{v}_\zeta - b(\zeta_\xi^+ + \zeta_\xi)) \rangle\rangle \tag{20}$$

where ζ^+ is such that $\boldsymbol{v}_\zeta \in G_{\zeta^+}$. Using this and the definition of $g(\cdot)$ it follows that the contribution of each term in the average (20) is non-negative. This proves that for a given $\boldsymbol{m} \in G_\zeta$ and $\boldsymbol{v}_\zeta = U\boldsymbol{m}$

$$E(\boldsymbol{m}) \geqslant Q_\zeta(\boldsymbol{v}_\zeta) \geqslant E(\boldsymbol{v}_\zeta) \tag{21}$$

which means that $E(\cdot)$ is indeed a Lyapunov function for the overlap dynamics (9). Note that equality is obtained if and only if $\boldsymbol{v}_\zeta \in G_\zeta$ which implies that $\boldsymbol{v}_\zeta$ is fixed.

We can now formulate an algorithm which visualizes the dynamics:

(1) Choose an initial overlap $\boldsymbol{m}$ in some region G_ζ characterized by a vector $\zeta \in \Sigma^{Q^p}$ such that $\zeta_\xi = g(\xi \cdot A\boldsymbol{m})$

(2) Compute $U\boldsymbol{m} = \boldsymbol{v}_\zeta = (1/C)\langle\langle \xi\zeta_\xi \rangle\rangle$.

(3) If $\boldsymbol{v}_\zeta \in G_\zeta$

then $\boldsymbol{v}_\zeta$ is a fixed point (the only one in G_ζ!)

else

- There is no fixed point in G_ζ.
- $E(\boldsymbol{v}_\zeta) < E(\boldsymbol{m})$.
- Repeat (1).

Thus we can conclude that a region G_ζ contains a fixed point if and only if

$$\forall \xi \in \Sigma^p: \quad g\left(\frac{1}{C}\langle\langle \xi \cdot A\xi'\zeta_{\xi'}\rangle\rangle\right) = \zeta_\xi. \tag{22}$$

This result provides us with a method for finding (in principle) all the fixed points of the dynamics: all ζ that satisfy (22) define a region that contains a fixed point, namely

$$v_\zeta = \frac{1}{C}\langle\langle \xi\zeta_\xi\rangle\rangle. \tag{23}$$

Although there is a restriction on the ζ to be tested ($\zeta_\xi = \zeta_{-\xi}$), in practice the algorithm is only useful for small p since the number of possible ζ is of the order $Q^{(Q^p/2)}$.

As an illustration we explicitly analyse the structure of the fixed points in the $Q=3$ model with $A=1$. In that case the saddle-point equation (5) can be written

$$m^\mu = \frac{1}{3^{p-1}}\sum_{\tilde\xi} g(m^\mu + \tilde\xi \cdot \tilde m_\mu) \tag{24}$$

with $\tilde\xi = (\xi^1, \ldots, \xi^{\mu-1}, \xi^{\mu+1}, \ldots, \xi^p)$ and $\tilde m_\mu = (m^1, \ldots, m^{\mu-1}, m^{\mu+1}, \ldots, m^p)$. Since $g(\cdot)$ now takes values in $\{-1, 0, +1\}$, we observe that every component has to be a multiple of $1/3^{p-1}$. Note that for the $Q=3$ case the overlap satisfies $|m^\mu| \leqslant 1$. Ordering the components of the overlap from high to low reduces the number of cases to be examined to $(3^{p-1}+1)!/(3^{p-1}-p+1)!$. This is much less than the number of cases in general, i.e. $3^{(3^p-1)/2}$.

For $p=2$, we then only have to consider the first octant of the (m^1, m^2) plane, leading to the following results:

- Because of (24) all fixed points satisfy $m^1 + m^2 \leqslant \frac{4}{3}$.
- The state $\boldsymbol{m} = (0, 0)$ is always a fixed point.
- For $0 < b < \frac{1}{3}$ there exists one retrieval state $(1, 0)$, one symmetric state $(\frac{2}{3}, \frac{2}{3})$ and one asymmetric state $(1, \frac{1}{3})$.
- For $\frac{1}{3} \leqslant b < \frac{2}{3}$ there exists one retrieval state $(1, 0)$, two symmetric states $(\frac{1}{3}, \frac{1}{3})$ and $(\frac{2}{3}, \frac{2}{3})$ and one asymmetric state $(\frac{2}{3}, \frac{1}{3})$.
- For $\frac{2}{3} \leqslant b < 1$ there is one retrieval state $(1, 0)$.
- For $1 \leqslant b$ there is no other fixed point but $(0, 0)$.

It is worth noting that the retrieval state appearing for $0 < b < 1$ is ground state only for $\frac{1}{6} < b \leqslant \frac{1}{2}$, as can be verified by explicitly computing the free energy (4). For general $Q > 3$ retrieval states only appear in a restricted region for b, namely

$$\frac{Q-3}{Q-2} < 2b \leqslant \frac{Q-1}{Q-2}. \tag{25}$$

4. Finite temperature dynamics

4.1. The flow equations

In order to find out how an arbitrary initial state of the system characterized by its overlap $\boldsymbol{m}$ changes in time, we derive the flow equations for the overlap using techniques similar to the two-state case [22, 23]. In contrast to the Potts model [20] we do not need to introduce sublattices.

We start from the symmetric learning rule (2). Suppose that the state of the network at time t is $\boldsymbol{\sigma}$ with $\sigma(i)=s_l$ from some $l\in\{1,\ldots,Q\}$. The probability that, at $t+\mathrm{d}t$, the ith neuron changes its state to $F_i^k s_l = s_{((l+k) \bmod Q)+1}$ is taken to be

$$w_i(s_l \to F_i^k s_l) = \frac{1}{Z_i}\exp\left[\frac{1}{T}(h_i(\boldsymbol{\sigma})F_i^k s_l - b(F_i^k s_l)^2)\right]$$
$$Z_i = \sum_{k=1}^{Q}\exp\left[\frac{1}{T}(h_i(\boldsymbol{\sigma})s_k - bs_k^2)\right]. \tag{26}$$

These transitions satisfy detailed balance. At this point it is important to remark that the limit $T\to 0$ of the dynamics described by these equations (26) (denoted in the following by $T=0^+$) is defined for continuous time, while the deterministic zero temperature dynamics given by (6) is defined for discrete time. Consequently, the solutions of the respective dynamical equations are not necessarily the same as we will see explicitly in section 4.2.

We then consider the probability $p(\boldsymbol{\sigma}, t)$ of observing the network in a state $\boldsymbol{\sigma}$ at time t. The following master equation is valid:

$$\frac{\partial p(\boldsymbol{\sigma}, t)}{\partial t} = \sum_{i=1}^{N}\sum_{k=1}^{Q}\{w_i(F_i^{-k}\sigma(i)\to\sigma(i))p(F_i^{-k}\boldsymbol{\sigma}, t) - w_i(\sigma(i)\to F_i^k\sigma(i))p(\boldsymbol{\sigma}, t)\}. \tag{27}$$

Defining the probability of finding the system at time t in a state with overlap $\boldsymbol{m}$ by

$$P(\boldsymbol{m}, t) = \sum_{\boldsymbol{\sigma}} p(\boldsymbol{\sigma}, t)\delta(\boldsymbol{m}-\boldsymbol{m}(\boldsymbol{\sigma})) \tag{28}$$

the master equation (27) transforms into

$$\frac{\partial P(\boldsymbol{m}, t)}{\partial t} = \sum_{\boldsymbol{\sigma}} p(\boldsymbol{\sigma}, t)\sum_{i=1}^{N}\sum_{k=1}^{Q} w_i(\sigma(i)\to F_i^k\sigma(i))$$
$$\times\left[\delta\left(\boldsymbol{m}-\boldsymbol{m}(\boldsymbol{\sigma})+\frac{1}{NC}\boldsymbol{\xi}_i\Delta_i^k(\boldsymbol{\sigma})\right)-\delta(\boldsymbol{m}-\boldsymbol{m}(\boldsymbol{\sigma}))\right] \tag{29}$$

with

$$\Delta_i^k(\boldsymbol{\sigma}) = \sigma(i) - F_i^k\sigma(i) \tag{30}$$

where we have used that

$$\boldsymbol{m}(\boldsymbol{\sigma}) - \boldsymbol{m}(F_i^k\boldsymbol{\sigma}) = \frac{1}{NC}\boldsymbol{\xi}_i\Delta_i^k(\boldsymbol{\sigma}). \tag{31}$$

Defining the average at time t of a test function $\Phi(\cdot)$ as

$$\bar{\Phi}_t \equiv \int \mathrm{d}\boldsymbol{m}\, P(\boldsymbol{m}, t)\Phi(\boldsymbol{m}) \tag{32}$$

we then arrive at

$$\frac{\mathrm{d}}{\mathrm{d}t}\bar{\Phi}_t = \int \mathrm{d}\boldsymbol{m}\frac{\partial P(\boldsymbol{m}, t)}{\partial t}\Phi(\boldsymbol{m}) \tag{33}$$

$$= \sum_{\boldsymbol{\sigma}}\int \mathrm{d}\boldsymbol{m}\,\delta(\boldsymbol{m}-\boldsymbol{m}(\boldsymbol{\sigma}))p(\boldsymbol{\sigma}, t)\sum_{i=1}^{N}\sum_{k=1}^{Q} w_i(\sigma(i)\to F_i^k\sigma(i))$$
$$\times\left[\Phi\left(\boldsymbol{m}(\boldsymbol{\sigma})-\frac{1}{NC}\boldsymbol{\xi}_i\Delta_i^k(\boldsymbol{\sigma})\right)-\Phi(\boldsymbol{m}(\boldsymbol{\sigma}))\right]. \tag{34}$$

Expanding the function Φ in powers of $1/N$, doing a partial integration and comparing with (33), we get

$$\frac{\partial P(\boldsymbol{m}, t)}{\partial t} = \nabla \cdot \left[P(\boldsymbol{m}, t) \left(\boldsymbol{m} - \frac{1}{C} \langle\!\langle \boldsymbol{\xi} \langle s \rangle \rangle\!\rangle \right) \right] + O(p^2/N) \tag{35}$$

where $\langle \cdot \rangle$ denotes a thermal average, i.e.

$$\langle f(s) \rangle = \frac{\sum_{k=1}^{Q} f(s_k) \exp[(1/T)(\boldsymbol{\xi} \cdot A\boldsymbol{m}s_k - bs_k^2)]}{\sum_{k=1}^{Q} \exp[(1/T)(\boldsymbol{\xi} \cdot A\boldsymbol{m}s_k - bs_k^2)]}. \tag{36}$$

Taking as initial probability distribution

$$P(\boldsymbol{m}, 0) = \delta(\boldsymbol{m} - \boldsymbol{m}_0) \tag{37}$$

the solution of (35) at time t reads

$$P(\boldsymbol{m}, t) = \delta(\boldsymbol{m} - \boldsymbol{m}(t)) \tag{38}$$

where the flow $\boldsymbol{m}(t)$ satisfies

$$\frac{\mathrm{d}\boldsymbol{m}(t)}{\mathrm{d}t} = -\boldsymbol{m} + \frac{1}{C} \langle\!\langle \boldsymbol{\xi} \langle s \rangle \rangle\!\rangle \tag{39}$$

with initial condition $\boldsymbol{m}(0) = \boldsymbol{m}_0$. So, comparing (5) and (39) we conclude that thermodynamical and dynamical stability are equivalent for invertible symmetric A. Furthermore, if A is strictly positive it follows that the free energy (4) is a Lyapunov function:

$$\frac{\mathrm{d}F(T, \boldsymbol{m}(t))}{\mathrm{d}t} = \sum_{\mu=1}^{p} \frac{\mathrm{d}m^{\mu}(t)}{\mathrm{d}t} \frac{\partial F(T, \boldsymbol{m})}{\partial m^{\mu}} = -\frac{1}{C} \frac{\mathrm{d}\boldsymbol{m}(t)}{\mathrm{d}t} \cdot A \frac{\mathrm{d}\boldsymbol{m}(t)}{\mathrm{d}t} < 0. \tag{40}$$

In order to study the stability properties of the state $\boldsymbol{m}$ one has to look at the eigenvalues of the matrix

$$S_{\mu\nu}(\boldsymbol{m}) = C\delta_{\mu,\nu} - \frac{1}{T} \langle\!\langle \xi^{\mu} (A\boldsymbol{\xi})^{\nu} (\langle s^2 \rangle - \langle s \rangle^2) \rangle\!\rangle \tag{41}$$

where $\langle s^2 \rangle$ and $\langle s \rangle$ are given by (36).

4.2. Stability properties for $Q = 3$ and $p = 2$

We use the flow equations (39) for the overlap to illustrate the complex behaviour of a multi-state model. We restrict ourselves to the most simple case: the $Q = 3$ model with $p = 2$ patterns and with synaptic matrix A taken to be the unit matrix. In this discussion it is useful to define the following function:

$$g(x) = \frac{1 + \gamma \cosh(x/T)}{3T[\gamma + \cosh(x/T)]^2} \qquad \gamma = \tfrac{1}{2} \exp(b/T). \tag{42}$$

We recall that it is sufficient to discuss the situation in the first octant since interchanging components or changing the sign of one of the components has no influence on the existence and nature of the fixed points.

4.2.1. The zero solution. The zero solution $m=(0,0)$ is always a fixed point. The stability of this point is determined by the eigenvalue λ of the stability matrix (41):

$$\lambda=-1+3g(0). \tag{43}$$

As we can see in figure 1 this splits the (b, T) plane in two regions separated by a line T_0: the zero state is stable in region I and unstable in region II. We observe that for $b>0.4631$ the zero solution is stable at any temperature.

4.2.2. Retrieval states. The solutions of the fixed-point equation (5) of the form $(m, 0)$ are given by

$$m=\frac{\sinh(m/T)}{\gamma+\cosh(m/T)}. \tag{44}$$

Studying the eigenvalues λ_1 and λ_2 of the corresponding stability matrix,

$$\lambda_1=-1+3g(m) \qquad \lambda_2=\lambda_1+g(0)-g(m) \tag{45}$$

we arrive at the situation depicted in figure 2.

At $T=0^+$ we find the stable retrieval state $m=1$ already mentioned in section 3. Furthermore, a repelling state $m=b$ occurs. Depending on b the behaviour of these states for increasing temperature is different.

For $0<b<0.4621$ the repelling respectively the retrieval state goes continuously to the zero state at T_0 respectively T_M. In the region enclosed by T_M^u the retrieval state becomes unstable due to the existence of a stable asymmetric state.

In the region $0.4621<b<0.4631$ there is re-entrant behaviour (see figure 5): the repelling state first goes continuously to the zero state which becomes unstable at the lower part of T_0. Then it continuously reappears at the higher part of T_0 where the zero state regains its stability. Finally it disappears discontinuously together with the retrieval state at T_M.

For $0.4631<b<1$ both states coalesce at T_M where they disappear, which is again reminiscent of a first order phase transition.

For $b\geq 1$ no solutions of the form $(m, 0)$, $m\neq 0$ exist.

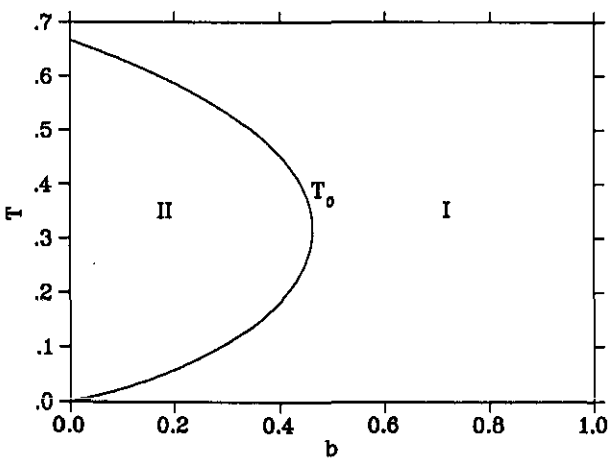

Figure 1. The temperature T_0 as a function of the parameter b for the $Q=3$, $p=2$ network. Region I: stable zero state; Region II: unstable zero state.

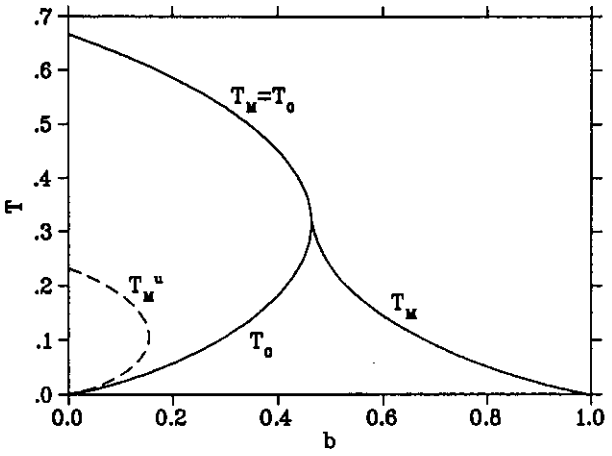

Figure 2. The temperatures T_M^u (dashed line), T_0 and T_M as a function of the parameter b for the $Q=3$, $p=2$ network. For $0<b<0.4621$, $T_0=T_M$. Within the region enclosed by the dashed curve T_M^u no stable retrieval state is possible.

4.2.3. The symmetric states. The solutions of the fixed-point equation (5) of the form (m, m) are determined from

$$m=\frac{1}{3}\left(\frac{\sinh(m/T)}{\gamma+\cosh(m/T)}+\frac{\sinh(2m/T)}{\gamma+\cosh(2m/T)}\right). \tag{46}$$

Studying the eigenvalues of the stability matrix,

$$\lambda_1=-1+g(m)+2g(2m) \qquad \lambda_2=-1+g(m)+2g(0) \tag{47}$$

we find the situation shown in figure 3.

At $T=0^+$ there exist, depending on b, stable symmetric states as discussed in section 3. Moreover, for $0<b<\frac{2}{3}$ a symmetric saddle-point occurs at $m=b/2$ and for $\frac{1}{3}<b<\frac{2}{3}$ a repelling symmetric point occurs at $m=b$. Depending on b and with increasing temperature the following behaviour is observed.

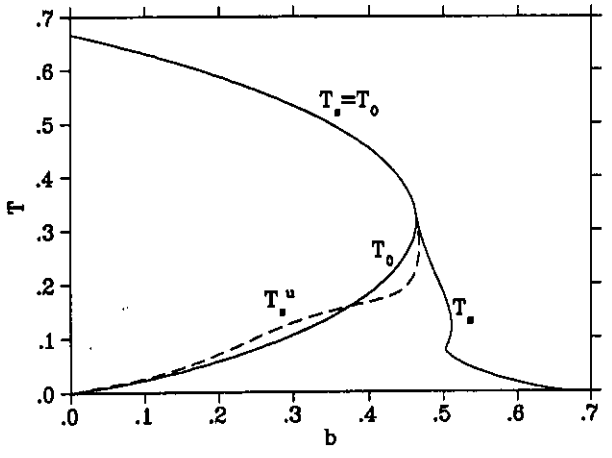

Figure 3. The temperatures T_s^u (dashed line), T_0 and T_s as a function of the parameter b for the $Q=3$, $p=2$ network. For $0<b<0.4621$, $T_0=T_s$.

For $0<b<\frac{1}{3}$ the lowest symmetric state goes continuously to the zero solution at $T=T_0$. The highest symmetric state is stable from $T=0$ to $T=T_s^u$. There it becomes a saddle-point going continuously to the zero solution at $T=T_s=T_M$.

For $\frac{1}{3}<b<\frac{2}{3}$ there are (at low temperatures) four symmetric states. Because the very existence of four symmetric states does not influence the retrieval properties of the network we only remark that at some still rather low temperature two of them disappear together.

- In the region $\frac{1}{3}<b<0.4621$ the behaviour is then similar as for $b<\frac{1}{3}$, once two of the four symmetric solutions have disappeared.
- For $0.4621<b<0.4631$, however, there are again re-entrance phenomena (see figure 5). At the lower part of T_s^u the highest symmetric state turns into a saddle-point and at the lower part of T_0 the lowest one continuously disappears in the zero solution making the latter unstable. At the higher part of T_0, however, the lowest state reappears. At the higher part of T_s^u the highest symmetric state regains its stability. Finally, at T_s the symmetric states coalesce and disappear.
- For $0.4631<b<0.4667$ only the re-entrance for T_s^u remains.
- In the region $0.4667<b<\frac{2}{3}$ the last two symmetric states coalesce at T_s where they disappear. However, for $0.5024<b<0.5114$ there is a re-entrance phenomenon. This is related to the fact that it is not always the same symmetric states that disappear first.

For $b>\frac{2}{3}$ there are no symmetric states.

4.2.4. The asymmetric states. In order to find the asymmetric states one has to solve the fixed-point equations (5) in general. The most important aspects of the behaviour of these asymmetric solutions are depicted in figure 4.

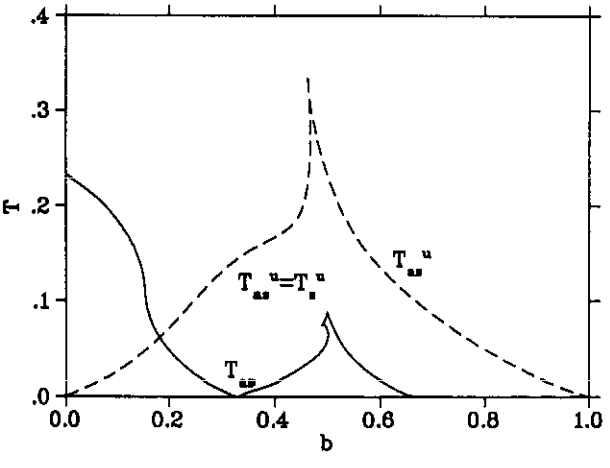

Figure 4. The temperatures T_{as}^u (dashed line) and T_{as} as a function of the parameter b for the $Q=3$, $p=2$ network. For $0<b<0.1547$, $T_{as}=T_M^u$. For $0<b<0.4621$, $T_{as}^u=T_s^u$.

In the region $0<b<\frac{1}{3}$ there exists at $T=0^+$ a stable state $(1,\frac{1}{3})$, a repelling state $(1,b)$ and a saddle-point $(\frac{2}{3}+\frac{1}{2}b,\frac{2}{3}-\frac{1}{2}b)$. With increasing T the saddle-point goes continuously to the highest symmetric state at T_s^u and turns this state into a saddle-point. For $0<b<0.1547$ the repelling state goes continuously to the retrieval state at T_M^u

and turns the latter into a saddle-point. However, for $0.1547 < b < \frac{1}{3}$ the repelling and attracting states coalesce at T_{as} where they disappear.

In the region $\frac{1}{3} < b < \frac{2}{3}$ the situation is more complicated. At $T = 0^+$ there is an attracting state $(\frac{2}{3}, \frac{1}{3})$. Furthermore, for $\frac{1}{3} < b < \frac{4}{9}$ there are at $T = 0^+$ four saddle-points $((1+b)/2, (1-b)/2)$, $(b, \frac{1}{3})$, $(\frac{2}{3}, b)$ and $(\frac{2}{3}+\frac{1}{2}b, \frac{2}{3}-\frac{1}{2}b)$, and one repelling point $(2b, b)$. However, for $\frac{4}{9} < b < \frac{2}{3}$ only the first three saddle-points solve (5).

In figure 4 we have indicated all information about the asymmetric states that is necessary to evaluate the retrieval qualities of the network:

- The attracting state mentioned above disappears together with one of the saddle-points at T_{as}. A complex re-entrance phenomenon can be observed for $0.4883 < b < 0.5000$.
- There exists an asymmetric saddle-point up to T_{as}^u. The leftmost part of T_{as}^u coincides with T_s^u. At this line the asymmetric saddle-point and the highest symmetric state coalesce turning the latter into a saddle-point. Consequently, in the region $0.4621 < b < 0.4667$ a re-entrance phenomenon corresponding to the one for T_s^u is observed (see figure 5). At the rightmost part of T_{as}^u the asymmetric saddle-point and the repelling solution to (44) coalesce turning the latter into a saddle-point.

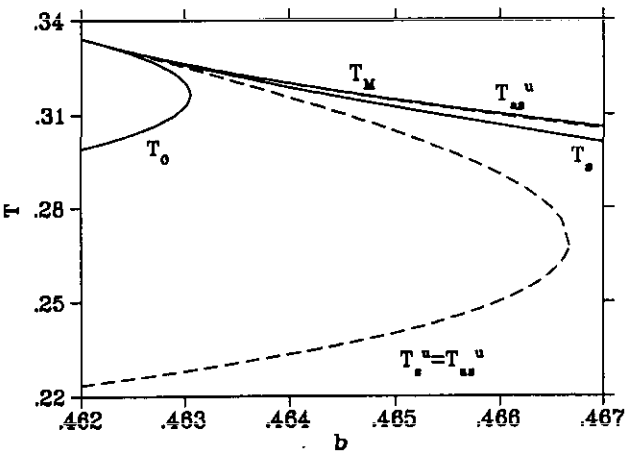

Figure 5. Re-entrant behaviour for $0.4621 < b < 0.4667$. The lines T_0, T_M, T_s, T_s^u and T_{as}^u are defined as before.

Finally, in the region $\frac{2}{3} < b < 1$ only one asymmetric state exists, namely the one corresponding to $((1+b)/2, (1-b)/2)$ at $T = 0^+$. It disappears continuously in the lowest retrieval state at T_{as}^u, turning the latter into a saddle-point.

It would be interesting to see if the features presented above survive for extensive loading α, which has, of course, to be studied with different methods. For the Hopfield model [17] for example (where it should be remarked that no parameter b is present) one knows that for finite α the system behaves in the retrieval regime very much as if it were at a finite temperature proportional to $(\alpha)^{1/2}$. Consequently the overlap will not be unity. However this overlap does not go continuously to zero with increasing temperature (i.e. a first-order transition occurs). Furthermore, for that model the spin-glass states appearing for finite α can be considered as the collective remnant of the finite-p symmetric mixture states.

4.3. Limit-cycle behaviour

Extending the learning rule (2) to asymmetric matrices A, the Hamiltonian formalism is no longer valid. However, one can easily show that the derivation of the dynamical equation (39) still goes through. In this case limit-cycle behaviour is possible. This phenomenon has already been observed for the Hopfield model [19] and the Potts model [20, 21]. We restrict ourselves here to an explicit example: $Q=3$, $p=2$, $b=0.3$ and the matrix A given by $A_{11}=A_{22}=1$, $A_{12}=-A_{21}=0.25$.

At $T=0^+$ there are four attracting and four repelling asymmetric points. The zero solution is stable.

When the temperature increases (see figure 6(a) with $T=0.04$) there exist four repelling asymmetric points and an attracting limit-cycle. The zero solution is stable.

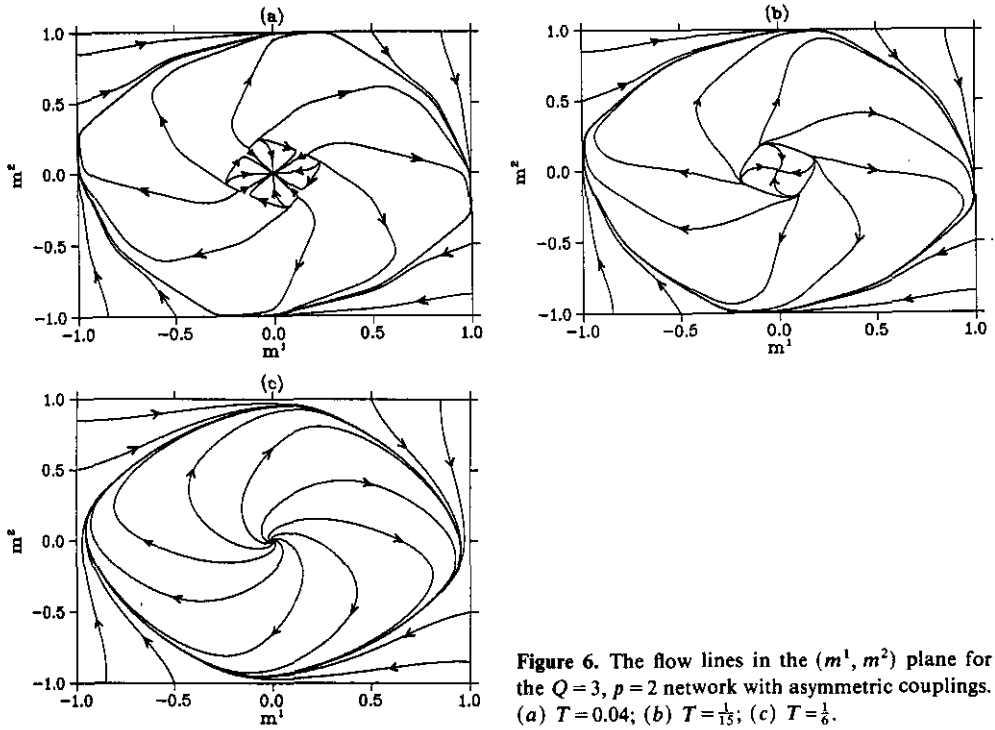

Figure 6. The flow lines in the (m^1, m^2) plane for the $Q=3$, $p=2$ network with asymmetric couplings. (a) $T=0.04$; (b) $T=\frac{1}{15}$; (c) $T=\frac{1}{6}$.

A further increase of the temperature (see figure 6(b) with $T=\frac{1}{15}$) results in the existence of one attracting and one repelling limit-cycle. The zero solution is stable.

The repelling limit-cycle contracts to zero and the zero solution becomes unstable when raising the temperature still further. The attracting limit-cycle remains (see figure 6(c) with $T=\frac{1}{6}$).

Finally, the attracting limit-cycle contracts to zero at $T=0.1063$ and the zero state becomes attracting. From here onwards this is the only remaining fixed point.

It is interesting to note that limit-cycle behaviour was also observed for the $Q=3$, $p=3$ system with the same values for the parameters b and T.

5. Concluding remarks

In this paper we have studied the dynamics of Q-Ising spin-glass neural networks with

a finite number of patterns at arbitrary temperature. In particular the existence and stability properties of the retrieval states and the spurious symmetric and asymmetric states were discussed. In this way we have not only better understood the retrieval properties of these attractor neural networks but we also gained some insight into the non-trivial dynamics of Q-Ising spins.

Allowing self-coupling between the neurons, we were able to show that for symmetric couplings satisfying a certain positivity condition (i.e. A strictly positive), there exists a Lyapunov function for the dynamics in the space of overlap vectors. In the zero-temperature case this could be used to construct an algorithm that allows, in principle, all the fixed points to be found. For practical reasons the number of neuron states and patterns should be small. Even in the simple example $Q=3$, $p=2$, $A=1$ there appeared, besides the retrieval states, symmetric and/or asymmetric states depending on the relative importance of the low (in absolute value) neuron states.

For finite temperature we have derived the flow equations for the overlap for couplings which need not be symmetric. We have then noticed that the thermodynamical and dynamical stability are equivalent for symmetric couplings. Studying the stability properties of the $Q=3$, $p=2$, $A=1$ model in detail gave us already a good illustration of the complex behaviour of these types of network. The (retrieval) performance of the network is strongly dependent upon the temperature and the parameter b, measuring the importance of the low neuron states. In fact for $0.4631 < b < 1$ the retrieval state is never the only attracting point of the dynamics. So the size of the basin of attraction is diminished by the existence of a repelling solution to the fixed-point equation for the overlap (cf (5)) and by the existence of an asymmetric saddle-point for temperatures up to T_{as}^{u}. For $0 < b < 0.4631$, however, situations do occur at sufficiently high temperatures where only the retrieval state is an attractor. Its basin of attraction is then, of course, maximal. We end with the remark that all states show re-entrant behaviour in the region $0.4621 < b < 0.4631$.

Acknowledgments

This work has been supported in part by the Research Fund of the Katholieke Universiteit Leuven (grant OT/91/13). One of the authors (DB) thanks the Belgian National Fund for Scientific Research for support as a Research Director.

References

[1] Kanter I 1988 *Phys. Rev.* A **37** 2739
[2] Noest A J 1988 *Phys. Rev.* A **38** 2196
[3] Cook J 1989 *J. Phys. A: Math. Gen.* **22** 2057
[4] Meunier C, Hansel D and Verga A 1989 *J. Stat. Phys.* **55** 859
[5] Yedidia J S 1989 *J. Phys. A: Math. Gen.* **22** 2265
[6] Stark J and Bressloff P 1990 *J. Phys. A: Math. Gen.* **23** 1633
[7] Rieger H 1990 *J. Phys. A: Math. Gen.* **23** L1273
[8] Rieger H 1990 *Statistical Mechanics of Neural Networks* (*Lecture Notes in Physics* **368**) ed L Garrido (Berlin: Springer) p 33
[9] Bollé D, Dupont P and van Mourik J 1991 *J. Phys. A: Math. Gen.* **24** 1065
[10] Bollé D and Dupont P 1990 *Statistical Mechanics of Neural Networks* (*Lecture Notes in Physics* **368**) ed L Garrido (Berlin: Springer) p 365
[11] Bollé D, Dupont P and van Mourik J 1991 *Europhys. Lett.* **15** 893; 1992 *Physica* A to appear

[12] Mertens S, Köhler H M and Bös S 1991 *J. Phys. A: Math. Gen.* **24** 4941
[13] Patrick A E, Picco P, Ruiz J and Zagrebnov V A 1991 *J. Phys. A: Math. Gen.* **24** L637
[14] Kohring G A 1991 *J. Stat. Phys.* **62** 563
[15] Gayrard V 1991 *Preprint CPT-91/P.2565* Marseille
[16] Shim G M, Kim D and Choi Y M 1992 *Phys. Rev.* A **45** 1238
[17] Amit D J, Gutfreund H and Sompolinsky H 1985 *Phys. Rev.* A **32** 1007
[18] Procesi C and Tirozzi B 1990 *Int. J. Mod. Phys.* B **4** 143
[19] Coolen A C C and Ruijgrok Th W 1988 *Phys. Rev.* A **38** 4253
[20] Bollé D and Mallezie F 1989 *J. Phys. A: Math. Gen.* **22** 4409
[21] Bollé D, Dupont P and Mallezie F 1989 *Neural Networks and Spin Glasses* ed W K Theumann and R Koeberle (Singapore: World Scientific) p 151
[22] Coolen A C C 1990 *Statistical Mechanics of Neural Networks* (*Lecture Notes in Physics* **368**) ed L Garrido (Berlin: Springer) p 381
[23] Riedel U, Kühn R and van Hemmen J L 1988 *Phys. Rev.* A **38** 1105